Pathology - Research and Practice 215 (2019) 152441

Contents lists available at ScienceDirect

Pathology - Research and Practice

journal homepage: www.elsevier.com/locate/prp

Histopathologic characteristics of advanced-stage *ROS1*-rearranged non-small cell lung cancers

Eunhyang Park[a,b], Yoon-La Choi[a], Myung-Ju Ahn[c], Joungho Han[a,*]

[a] Department of Pathology and Translational Genomics, Samsung Medical Center, Sungkyunkwan University School of Medicine, Seoul, Republic of Korea
[b] Department of Pathology, Yonsei University College of Medicine, Seoul, Republic of Korea
[c] Division of Hematology-Oncology, Department of Medicine, Samsung Medical Center, Sungkyunkwan University School of Medicine, Seoul, Republic of Korea

ARTICLE INFO

Keywords:
ROS1
FISH
Histology
Non-small cell lung cancer (NSCLC)
Lung adenocarcinoma
Immunohistochemistry

ABSTRACT

Background: *ROS1* rearrangement accounts for 1%–2% of non-small cell lung cancer (NSCLC) with a remarkable response to crizotinib. Although *ROS1*-rearranged tumors are known to have characteristic histologic features, only a few studies have investigated the histologic features of advanced-stage ROS1-rearranged tumors.

Methods: We analyzed the histopathologic features of *ROS1*-rearranged tumors in advanced-stage NSCLC patients and assessed the ROS1 immunohistochemistry (IHC) staining patterns of *ROS1*-rearranged cases.

Results: A total of 37 *ROS1* fluorescence in situ hybridization (FISH)-positive cases and 64 *ROS1* FISH-negative cases were analyzed, and all tumors were *EGFR*-, *ALK*-, and *RET*-negative. Solid pattern, round nuclei with macronucleoli, solid signet-ring cells, extracellular mucin, and a close relation with adjacent bronchioles were significantly associated with *ROS1* rearrangement, and the solid signet-ring cell feature was exclusively identified in *ROS1*-rearranged tumors. ROS1 IHC showed a 97.3% sensitivity when weak to strong protein expression was considered positive.

Conclusions: Our findings highlight distinct histologic features of *ROS1*-rearranged tumors, including their nuclear features. A thorough understanding of *ROS1* rearrangement-related histologic features would be helpful to identify *ROS1*-rearranged tumors in advanced-stage NSCLC.

1. Introduction

In the last decade, non-small cell lung cancer (NSCLC) has achieved a great paradigm shift due to oncogenic drivers and their response towards targeted therapy. The most representative targets for NSCLC are *EGFR* and anaplastic lymphoma kinase (*ALK*), which account for 30% and 3% of NSCLC cases, respectively [1,2]. Subsequently, the identification of novel mutations became crucial to determine the treatment strategy and predict the prognosis of NSCLC patients. Recently, oncogenic fusions of *ROS1, RET*, and *NTRK1* have emerged as noteworthy targets [3–5]. Despite their rarity, they show a notable therapeutic response to tyrosine kinase inhibitors; hence, these genetic alterations must not be missed for the treatment of patients. Generally, these oncogenic drivers are mutually exclusive [6,7]; this makes it necessary to conduct a thorough and comprehensive testing of rare oncogenic drivers in wild-type *EGFR* and *ALK* NSCLC patients.

Among these, *ROS1* rearrangement accounts for 1%–2% of NSCLC cases with a remarkable response to crizotinib [3,8,9]. Patients with *ROS1*-rearranged tumors are prone to be younger and never smokers, and have an adenocarcinoma histology, which are similar to *EGFR*-mutant and *ALK*-rearranged tumors [3]. Fluorescence in situ hybridization (FISH) is a gold standard method to detect *ROS1* rearrangement. However, high costs, the requirement for specialized equipment, and complex interpretation of the results have made it difficult to use FISH for testing all NSCLC patients. To compensate for these disadvantages, immunohistochemistry (IHC) test has been considered an effective screening method for detecting *ROS1* rearrangement, as being used for screening *ALK* rearrangement [10–15]. However, ROS1 IHC is associated with a high rate of false-positive results and difficulties in interpreting due to background staining [16].

On the other hand, previous studies had reported characteristic histological features of *ROS1*-rearranged NSCLC, such as solid signet-ring cells and mucinous-cribriform patterns [10–14,17]. Zhao et al. compared histologic features of *ROS1*-rearranged and *ROS1*-negative cases and declared that histologic features could be used as a pre-screening method to increase the specificity of the ROS1 IHC results [18,19]. However, because of the rarity of the *ROS1* rearrangement, only a few studies have investigated the histologic features of *ROS1*-

* Corresponding author.
E-mail address: hanjho@skku.edu (J. Han).

https://doi.org/10.1016/j.prp.2019.152441
Received 4 March 2019; Received in revised form 16 April 2019; Accepted 5 May 2019
0344-0338/ © 2019 Elsevier GmbH. All rights reserved.

rearranged tumors in a limited number of cases. Moreover, the known *ROS1* rearrangement-related histologic features are considered as high-grade architectural features which are frequently identified in advanced-stage adenocarcinoma [20–22]. Thus, in advanced-stage NSCLC, not all of the histologic features might be helpful to distinguish *ROS1*-rearranged tumors. Because of the particular importance of detecting oncogenic targets in advanced-stage NSCLC patients, it would be beneficial to identify distinguished histology of *ROS1*-rearranged tumors in advanced-stage NSCLC.

In this study, we analyzed the histopathologic features of *ROS1*-rearranged tumors and compared them to those of *ROS1*-negative tumors in a group of patients with advanced-stage NSCLC. We also assessed the ROS1 IHC staining patterns of *ROS1*-rearranged cases.

2. Materials and methods

2.1. Case selection

ROS1 FISH was tested in 454 advanced-stage NSCLC cases at the Samsung Medical Center from April 2013 to October 2018. Among them, 42 cases (9.3%) were FISH-positive, 368 cases (81.1%) were FISH-negative, and no results were obtained for 44 cases (9.6%) due to poor specimen quality or insufficient tumor volume. Patients with advanced stages of disease, i.e. stage III and IV, were enrolled. Of 42 FISH-positive cases, five cases were excluded as the specimens were obtained after neoadjuvant chemotherapy or radiation therapy. A total of 37 *ROS1* FISH-positive cases, consisting of 13 resection and 24 biopsy specimens, were analyzed. As the negative control group, 64 *ROS1* FISH-negative cases with 1) stage III and IV, 2) adenocarcinoma or tumor containing adenocarcinoma component, 3) wild-type *EGFR, ALK,* and *RET,* and 4) no history of neoadjuvant chemotherapy or radiation therapy before sampling, were selected. The cases included 24 resection and 40 biopsy specimens. This study was approved by the Institutional Review Board of the Samsung Medical Center (IRB No. 2018-11-126-001).

2.2. Histologic analysis

Hematoxylin and eosin (H&E)-stained slides were reviewed by two experienced pathologists (J.H. and E.P.) based on the 2015 World Health Organization (WHO) classification of lung adenocarcinoma [23]. Histologic features including previously reported characteristic patterns of *ROS1*-rearranged tumors were evaluated [10–14,17]. The features were divided into three subcategories; 1) architectural patterns, 2) cytologic features, and 3) others. Architectural patterns were determined as any presence of solid, cribriform (sheets of tumor cells with fenestrations), mucinous-cribriform (cribriform structure associated with abundant extracellular mucus), micropapillary, and lepidic patterns. Cytologic features including round nuclei with central macronucleoli, solid with signet-ring cells (solid growth pattern containing signet-ring cells), abundant eosinophilic cytoplasm, intracytoplasmic mucin, and bizarre cells were evaluated with a cut-off value of > 30% for tumor cells. Others category included extracellular mucin, psammomatous calcification, and a relation to adjacent bronchioles. A relation to adjacent bronchioles was evaluated whether tumor surrounds the bronchioles or tumor cells invaded to the adjacent bronchiolar epithelium in lung specimen.

2.3. ROS1 FISH detection

FISH analysis was performed on formalin-fixed paraffin-embedded (FFPE) tissue using POSEIDON *ROS1* Dual Color Break Apart Probe (Kreatech, Inc., Amsterdam, the Netherlands), and 50 non-overlapping nuclei were counted. Patients were considered *ROS1* positive, if there was a break-apart pattern with one fusion signal and two separate green and orange signals or an isolated green signal in at least 15% of tumor cells.

2.4. ROS1 IHC staining and scoring

FFPE tissues were sectioned at a thickness of 4-μm and stained with D4D6 rabbit monoclonal ROS1 antibody (Cell Signaling Technology, Danvers, MA, USA; 1:50 dilution) using the Leica Bond Max III automated system (Bond, Bannockburn, Illinois, USA). The detection was performed with the EnVision system (K4003, DAKO, Glostrup, Denmark), according to the manufacturer's protocol. Benign pneumocytes and alveolar macrophages were used as positive controls. The results were assessed using the H-score (range of total score: 0–300). The percentage of positive cells (0%–100%) was multiplied by each staining intensity (0, no appreciable staining; 1, barely detectable staining; 2, distinct brown staining; and 3, strong dark brown staining). In resection cases, staining pattern, i.e. whether the staining was homogenous or heterogenous, was investigated.

2.5. Analyses of EGFR mutation and ALK and RET rearrangement

EGFR mutations in the 18th, 19th, 20th, and 21 st exon were evaluated using real-time polymerase chain reaction after peptide nucleic acid (PNA)-clamping using the PNA clamping *EGFR* Mutation Detection Kit (Panagene, Inc., Daejeon, Korea). *ALK* FISH analysis was performed with the Vysis LSI *ALK* Dual Color Break Apart Probe (Abbott Molecular, Abbott Park, IL, USA). *RET* FISH test was performed using the ZytoLight SPEC *RET* Dual Color Break Apart Probe (ZytoVision GmbH, Bremerhaven, Germany). In the FISH analysis, 50 non-overlapping nuclei were counted and the detection of at least 15% of a split or isolated orange signal was regarded as a positive result.

2.6. Statistical analysis

A χ^2 test or Fisher's exact test was used to evaluate the statistical significance between two variables. The distribution of age was evaluated with the Shapiro-Wilk test. $p < 0.05$ was considered statistically significant for all analyses, and all analyses were two-sided. All data were analyzed using the R software.

3. Results

3.1. Clinical characteristics of ROS1-rearranged NSCLC

ROS1-rearranged group was significantly prone to be female and never smokers compared to *ROS1*-negative group. The average age was slightly younger in the *ROS1*-rearranged group, but not statistically significant. None of the tumors harbored concurrent *EGFR* mutation or *ALK* or *RET* rearrangement. There was no significant difference between the TNM stages in both groups. Clinicopathologic characteristics of *ROS1*-rearranged and *ROS1*-negative groups and detailed information of the *ROS1*-rearranged group are summarized in Table 1 and Table 2, respectively.

3.2. Histologic features of ROS1-rearranged NSCLC

ROS1-rearranged tumors included 94.6% of adenocarcinoma and 5.4% of pleomorphic carcinoma containing adenocarcinoma component. *ROS1*-negative tumors were composed of 85.9% of adenocarcinoma, 1.6% of adenosquamous carcinoma, and 12.5% of invasive mucinous carcinoma. Since invasive mucinous carcinoma is regarded to be a distinct variant of lung adenocarcinoma with unique histological and genetic feature (i.e. *KRAS* mutation), we excluded invasive mucinous adenocarcinoma in histologic comparison of *ROS1*-rearranged and *ROS1*-negative tumors. Instead, we additionally compared histologic features of *ROS1*-rearranged tumors and *ROS1*-negative invasive mucinous adenocarcinoma, since this variant poses a diagnostic challenge

Table 1
Clinicopathologic characteristics of *ROS1*-rearranged and *ROS1*-negative groups.

	ROS1-rearranged (n = 37)	*ROS1*-negative (n = 64)	*p*
Age, years			0.31
Average	56.3 +/− 11.1	58.7 +/− 11.6	
Range	33–78	32–81	
Sex			0.018
Male	11 (29.7%)	36 (56.2%)	
Female	26 (70.3%)	28 (43.7%)	
Smoking status			0.005
Never smoker	31 (83.8%)	33 (51.6%)	
Ex-smoker	3 (8.1%)	17 (26.6%)	
Current smoker	3 (8.1%)	14 (21.9%)	
Histology			0.031
Adenocarcinoma	35 (94.6%)	55 (85.9%)	
Adenoquamous carcinoma	0 (0.0%)	1 (1.6%)	
Pleomorphic carcinoma	2 (5.4%)	0 (0.0%)	
Invasive mucinous carcinoma	0 (0.0%)	8 (12.5%)	
Stage			0.159
IIIa	6 (16.2%)	3 (4.7%)	
IIIb	2 (5.4%)	6 (9.4%)	
IIIc	0 (0.0%)	2 (3.1%)	
IV	29 (78.4%)	53 (82.8%)	
Survival			0.272
Alive	20 (54.1%)	26 (40.6%)	
Expire	17 (45.9%)	38 (59.4%)	
Specimen type			0.981
Biopsy	24 (64.9%)	40 (62.5%)	
Resection	13 (35.1%)	24 (37.5%)	
Organ			0.011
Lung	24 (66.7%)	46 (71.9%)	
Lymph Node	8 (22.2%)	10 (15.6%)	
Pleura	2 (5.6%)	4 (6.2%)	
Distant Organ	2 (5.6%)	4 (6.2%)	

due to the overlapped mucinous feature with *ROS1*-rearranged tumors.

In histologic analysis, solid pattern, round nuclei with macronucleoli, solid-signet ring cells, extracellular mucin, and a close relation with adjacent bronchioles were more frequently identified in *ROS1*-rearranged tumors, than in *ROS1*-negative tumors ($p < 0.05$) (Table 3 and Fig. 1A–1E); the solid signet-ring cell feature was exclusively identified in the *ROS1*-rearranged tumors. Abundant eosinophilic cytoplasm was associated with *ROS1*-negative tumors. The lepidic pattern was not identified in both the groups.

In analysis of *ROS1*-rearranged tumors and invasive mucinous adenocarcinoma, mucinous cells or extracellular mucin was identified as a minor component in *ROS1*-rearranged tumors, while invasive mucinous adenocarcinomas were mainly composed of mucinous cells with abundant extracellular mucin. In addition, mucinous cells of *ROS1*-rearranged tumors presented with centrally placed, large round nuclei or signet-ring cells having crescent-shaped, peripherally displaced nuclei, while invasive mucinous adenocarcinomas were comprised of columnar cells with apical mucin and basally located, vesicular nuclei (Fig. 1F).

3.3. IHC results of ROS1-rearranged NSCLC

Among 37 *ROS1* FISH-positive cases, 36 cases (97.3%) showed ROS1 protein expression in the IHC staining analysis. Of these, 33 cases showed H-scores of > 250 and the remained three cases showed H-scores of 240, 130, and 40 (Fig. 2). There were 14 resection cases, of these, 13 cases showed diffuse homogenous staining patterns with a staining intensity of +2 to +3. One case (H-score = 40) showed heterogenous pattern with a staining intensity of 0 to +1.

4. Discussion

In this study, we attempted to identify *ROS1* rearrangement-related histologic features in a group of patients with advanced-stage NSCLC. As a result, solid pattern, round nuclei with macronucleoli, solid signet-ring cells, extracellular mucin, and a close relation with adjacent bronchioles were found to be significantly associated with *ROS1* rearrangement, and the solid signet-ring cell pattern was exclusively observed in *ROS1*-rearranged tumors. In addition, ROS1 IHC showed 97.3% sensitivity when weak to strong protein expression was considered as a positive result.

In *ROS1* FISH-tested cases, *ROS1* rearrangement was identified in 9.3%. This high proportion of *ROS1* FISH positivity is because *ROS1* FISH was tested in clinically selected cases with *EGFR/ALK* negative tumor or tumor with poor therapeutic response. Patients with *ROS1*-rearranged tumors were prone to be female and never smokers, and demonstrated an adenocarcinoma histology, which are consistent with previous studies [3,9].

In this study, round nuclei with macronucleoli were significantly associated with *ROS1*-rearranged tumors. On the other hand, a large portion of *ROS1*-negative tumors had vesicular tumor nuclei with multiple nucleoli. Similar histologic feature had been described in few studies as a “hepatoid cytology”, which indicated round nuclei, prominent nucleoli, and abundant eosinophilic cytoplasm [14,19], however, we analyzed the nuclear and cytoplasmic features separately and identified distinct nuclear feature of *ROS1*-rearranged tumors. Although the current WHO classification of lung adenocarcinoma does not recommend reporting nuclear features of the tumor in pathologic diagnosis [23], several studies demonstrated that nuclear features are significantly associated with prognosis in lung adenocarcinoma, suggesting the inclusion of the nuclear grading system in pathologic report [24–27]. Because the tumor nuclei contain genetic information of tumor cells, nuclear feature might reflect tumor characteristics and molecular alterations of tumors. Our finding suggests that the nuclear feature–round nuclei with macronucleoli would help to better detect *ROS1*-rearranged tumors.

Lung cancers harboring *ALK*, *ROS1*, and *RET* rearrangement had been considered to a distinct subgroup sharing similar histologic features [12,14], although the reason is unknown. In this study, *ROS1*-rearranged tumors exclusively harbored solid signet-ring cell feature and the tumors were prone to be closely related to adjacent bronchioles. These findings were also reported in *ALK*-rearranged adenocarcinoma and regarded as an evidence of distinct cells of origin–i.e. proximal, juxta-bronchial progenitors [28–30]. Thus, fusion gene-associated lung cancers may arise from distinct cells of origin which might result in overlapped histologic features. Further study is needed to reveal the origin of fusion gene-associated tumors and understand their pathogenesis.

Other histologic features, which were previously reported as characteristic patterns of *ROS1*-rearranged tumors, were not differently identified in advanced-stage *ROS1*-rearranged and *ROS1*-negative groups. These histologic features might not be the result of *ROS1* rearrangement but the result of tumor progression. However, previous studies reported some of these histologic features in early-stage *ROS1*-rearranged adenocarcinoma [11–15]. This implies that *ROS1*-rearranged tumors might have an aggressive behavior and rapidly progress to the advanced stage.

Because *ROS1*-rearranged tumors often present with extracellular mucin or signet-ring cells harboring mucin, they could be misdiagnosed as an invasive mucinous adenocarcinoma. However, we observed that the mucinous component of *ROS1*-rearranged tumors is focal, and they have centrally placed, large and round nuclei, which is distinct from invasive mucinous adenocarcinoma. *ROS1*-rearranged tumor and invasive mucinous adenocarcinoma have different genetic alterations and clinical courses that it is important to histologically distinguish these subtypes [31].

Table 2
Clinicopathologic details of *ROS1*-rearranged lung cancers.

Patient No.	Age (years)	Sex	Smoking	Diagnosis	TNM	Stage	Specimen type	Immunohistochemistry	
								Staining pattern	H-score
P1	66	M	NS	ADC	pT2aN3M1c	IV	Biopsy	NA	> 250
P2	35	F	NS	ADC	cT4N3M1c	IV	Biopsy	NA	> 250
P3	54	F	NS	ADC	pT4N0M1a	IV	Biopsy	NA	> 250
P4	59	F	NS	ADC	cT2bNxM1c	IV	Biopsy	NA	> 250
P5	52	M	ES	ADC	cT2aN2M1c	IV	Biopsy	NA	> 250
P6	54	F	NS	ADC	cT4N3M1c	IV	Biopsy	NA	> 250
P7	41	F	NS	ADC	cT4N1M1a	IV	Resection	Homogenous	> 250
P8	50	F	NS	ADC	cT4NxM1c	IV	Resection	Homogenous	> 250
P9	41	M	NS	ADC	cT4N2M1a	IV	Biopsy	NA	> 250
P10	52	F	NS	ADC	cT4N3M1c	IV	Biopsy	NA	> 250
P11	63	M	ES	ADC	pT1aN0M1a	IV	Resection	Homogenous	> 250
P12	73	F	NS	ADC	cTxN3M1c	IV	Biopsy	NA	> 250
P13	78	F	NS	ADC	cT2N3M1a	IV	Resection	Homogenous	> 250
P14	53	M	NS	ADC	pT1aN2M0	IIIA	Resection	Homogenous	210
P15	33	F	NS	ADC	cT2N2M1a	IV	Biopsy	NA	> 250
P16	74	F	NS	ADC	cTxN2M1c	IIIA	Resection	Homogenous	> 250
P17	53	F	NS	ADC	cT1bN3M1c	IV	Biopsy	NA	> 250
P18	58	F	NS	ADC	cT2aN3M1c	IV	Biopsy	NA	0
P19	61	M	NS	ADC	pT3N1M0	IIIA	Resection	Homogenous	> 250
P20	41	M	ES	Pleomorphic CA	cT4N3M1c	IV	Biopsy	NA	> 250
P21	58	F	NS	ADC	cT4N2M1c	IV	Biopsy	NA	> 250
P22	51	F	NS	ADC	cT1bN3M1a	IV	Biopsy	NA	> 250
P23	64	F	NS	ADC	cT2bN3M1a	IV	Biopsy	NA	> 250
P24	59	F	NS	ADC	cT2N2M1c	IV	Biopsy	NA	> 250
P25	57	M	CS	ADC	cT1bN3M0	IIIB	Biopsy	NA	> 250
P26	68	F	NS	ADC	cT2aN1M1c	IV	Biopsy	NA	> 250
P27	35	F	NS	Pleomorphic CA	pT2aN0M1c	IV	Resection	Homogenous	> 250
P28	60	M	NS	ADC	cT4N3M1c	IV	Biopsy	NA	> 250
P29	60	F	NS	ADC	cT4N0M0	IIIA	Biopsy	NA	> 250
P30	66	M	CS	ADC	cT1bN0M1b	IV	Resection	Heterogenous	40
P31	67	F	NS	ADC	cT4N3M1b	IV	Biopsy	NA	> 250
P32	70	F	NS	ADC	cT4N3M1b	IV	Resection	Homogenous	> 250
P33	65	F	NS	ADC	pT4N1M0	IIIA	Resection	Homogenous	> 250
P34	57	F	NS	ADC	cT4N2M0	IIIB	Biopsy	NA	130
P35	43	F	NS	ADC	cT2bN3M1c	IV	Biopsy	NA	> 250
P36	57	M	CS	ADC	pT2aN2M0	IIIA	Resection	Homogenous	> 250
P37	55	F	NS	ADC	cT4N2M1b	IV	Resection	Homogenous	> 250

Abbreviations: ADC, adenocarcinoma; CA, carcinoma; CS, current smoker; ES, ex-smoker; F, female; M, male; NS, never smoker; NA, not applicable.

Table 3
Histopathologic features of *ROS1*-rearranged and *ROS1*-negative lung cancers.

	ROS1-rearranged (n = 37)	*ROS1*-negative (n = 64)	*p*
Architectural patterns			
Solid	27 (73.0%)	27 (48.2%)	0.031
Cribriform	8 (21.6%)	16 (29.1%)	0.577
Mucinous-cribriform	3 (8.1%)	5 (8.9%)	1
Micropappillary	23 (62.2%)	30 (53.6%)	0.545
Lepidic	0 (0%)	0 (0%)	
Cytologic features			
Round nuclei with macronucleoli	27 (73.0%)	14 (25.0%)	< 0.001
Solid-signet ring cells	5 (13.5%)	0 (0.0%)	0.018
Abundant eosinophilic cytoplasm	20 (54.1%)	43 (76.8%)	0.039
Intracytoplasmic mucin	4 (10.8%)	5 (8.9%)	1
Bizarre cells	18 (48.6%)	22 (39.3%)	0.497
Others			
Extracellular mucin	8 (21.6%)	3 (5.4%)	0.040
Psammomatous calcification	6 (16.2%)	5 (8.9%)	0.461
In lung specimen	(n = 24)	(n = 46)	
Relation with adjacent bronchioles	14 (58.3%)	4 (8.7%)	< 0.001

Several studies validated ROS1 IHC with *ROS1* FISH or RT-PCR and suggested IHC as a highly sensitive screening tool for *ROS1* rearrangement [32,33]. We also observed 97.3% sensitivity of ROS1 IHC with mostly diffuse homogenous staining pattern. However, one case showed negative protein expression and one case showed focal weak protein expression. These discordant *ROS1* IHC-negative/focal weak positive and FISH-positive cases raised the possibility of false-negative IHC or false-positive FISH results. In IHC-negative case (P18), *ROS1* FISH showed split signals in 30% of tumor cells (15/50). The patient was treated with crizotinib, however, the tumor progressed to liver and multiple brain metastases. The other case with focal weak protein expression (P30) was positive for FISH with split signals (9/50) and isolated 3′ signals (6/50). Since the patient refused to be treated, the response to crizotinib could not be known. Poor crizotinib response of patient P18 suggests that the result of *ROS1* FISH might be false-positive. False-positive FISH results could be due to detection of non-functional fusions of unexpected points or fusions inactivated by post-translational modification. Discrepant IHC results could be a clue to consider re-validation of the results by orthogonal methods–RT-PCR or next-generation sequencing.

The limitation of this study is that biopsy specimens were included for the histologic analysis, which might not be representative of the tumor. The reason is that our study population consisted of a fair number of unresectable stage patients. In addition, discordant IHC-FISH cases imply the possibility of false-positive FISH results, as discussed above.

5. Conclusion

In this study, we evaluated a considerable number of *ROS1*-rearranged advanced-stage tumors and highlight distinct histologic features

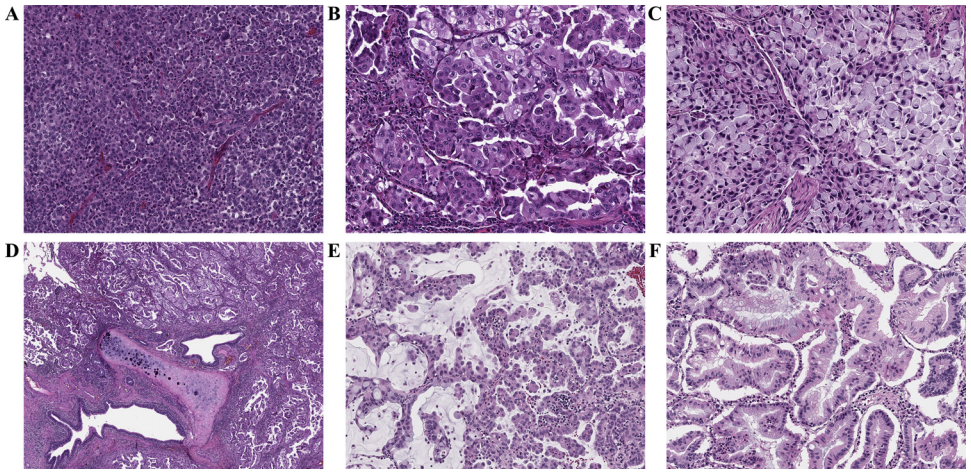

Fig. 1. Representative histologic features of *ROS1*-rearranged tumors and *ROS1*-negative invasive mucinous adenocarcinoma. (A), Solid pattern, (B), round nuclei with macronucleoli, (C), solid-signet ring cells, (D), close relation with adjacent bronchioles, and (E), extracellular mucin of *ROS1*-rearranged tumors. (F) Cytonuclear feature of *ROS1*-negative invasive mucinous adenocarcinoma.

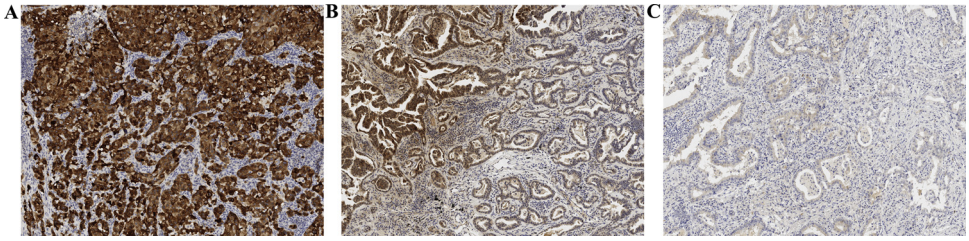

Fig. 2. Immunohistochemistry staining patterns of *ROS1*-rearranged tumors. (A), diffuse strong cytoplasmic staining (H-score > 250), (B), diffuse moderate cytoplasmic staining (H-score = 210), and (C), focal weak cytoplasmic staining (H-score = 40).

of *ROS1*-rearranged tumors including nuclear feature. Our findings also provide the evidence for understanding the cell of origin of fusion gene-associated lung cancers. A thorough understanding of *ROS1* rearrangement-related histologic features would be helpful to identify *ROS1*-rearranged tumors in advanced-stage NSCLC.

Conflicts of interest

All authors declare no conflicts of interest.

References

[1] E.L. Kwak, Y.-J. Bang, D.R. Camidge, A.T. Shaw, B. Solomon, R.G. Maki, S.-H.I. Ou, B.J. Dezube, P.A. Jänne, D.B. Costa, M. Varella-Garcia, W.-H. Kim, T.J. Lynch, P. Fidias, H. Stubbs, J.A. Engelman, L.V. Sequist, W. Tan, L. Gandhi, M. Mino-Kenudson, G.C. Wei, S.M. Shreeve, M.J. Ratain, J. Settleman, J.G. Christensen, D.A. Haber, K. Wilner, R. Salgia, G.I. Shapiro, J.W. Clark, A.J. Iafrate, Anaplastic lymphoma kinase inhibition in non–small-cell lung cancer, N. Engl. J. Med. 363 (2010) 1693–1703, https://doi.org/10.1056/NEJMoa1006448.

[2] T.J. Lynch, D.W. Bell, R. Sordella, S. Gurubhagavatula, R.A. Okimoto, B.W. Brannigan, P.L. Harris, S.M. Haserlat, J.G. Supko, F.G. Haluska, D.N. Louis, D.C. Christiani, J. Settleman, D.A. Haber, Activating mutations in the epidermal growth factor receptor underlying responsiveness of non–small-cell lung cancer to gefitinib, N. Engl. J. Med. 350 (2004) 2129–2139, https://doi.org/10.1056/NEJMoa040938.

[3] K. Bergethon, A.T. Shaw, S.H.I. Ou, R. Katayama, C.M. Lovly, N.T. McDonald, P.P. Massion, C. Siwak-Tapp, A. Gonzalez, R. Fang, E.J. Mark, J.M. Batten, H. Chen, K.D. Wilner, E.L. Kwak, J.W. Clark, D.P. Carbone, H. Ji, J.A. Engelman, M. Mino-Kenudson, W. Pao, A.J. Iafrate, ROS1 rearrangements define a unique molecular class of lung cancers, J. Clin. Oncol. 30 (2012) 863–870, https://doi.org/10.1200/JCO.2011.35.6345.

[4] R. Wang, H. Hu, Y. Pan, Y. Li, T. Ye, C. Li, X. Luo, L. Wang, H. Li, Y. Zhang, F. Li, Y. Lu, Q. Lu, J. Xu, D. Garfield, L. Shen, H. Ji, W. Pao, Y. Sun, H. Chen, RET fusions define a unique molecular and clinicopathologic subtype of non-small-cell lung cancer, J. Clin. Oncol. 30 (2012) 4352–4359, https://doi.org/10.1200/JCO.2012.44.1477.

[5] A. Vaishnavi, M. Capelletti, A.T. Le, S. Kako, M. Butaney, D. Ercan, S. Mahale, K.D. Davies, D.L. Aisner, A.B. Pilling, E.M. Berge, J. Kim, H. Sasaki, S. Park, G. Kryukov, L.A. Garraway, P.S. Hammerman, J. Haas, S.W. Andrews, D. Lipson, P.J. Stephens, V.A. Miller, M. Varella-Garcia, P.A. Jänne, R.C. Doebele, Oncogenic and drug-sensitive NTRK1 rearrangements in lung cancer, Nat. Med. 19 (2013) 1469–1472, https://doi.org/10.1038/nm.3352.

[6] J.J. Lin, L.L. Ritterhouse, S.M. Ali, M. Bailey, A.B. Schrock, J.F. Gainor, L.A. Ferris, M. Mino-Kenudson, V.A. Miller, A.J. Iafrate, J.K. Lennerz, A.T. Shaw, ROS1 fusions rarely overlap with other oncogenic drivers in non–small cell lung cancer, J. Thorac. Oncol. 12 (2017) 872–877, https://doi.org/10.1016/j.jtho.2017.01.004.

[7] J.F. Gainor, A.M. Varghese, S.-H.I. Ou, S. Kabraji, M.M. Awad, R. Katayama, A. Pawlak, M. Mino-Kenudson, B.Y. Yeap, G.J. Riely, A.J. Iafrate, M.E. Arcila, M. Ladanyi, J.A. Engelman, D. Dias-Santagata, A.T. Shaw, ALK rearrangements are mutually exclusive with mutations in EGFR or KRAS: an analysis of 1,683 patients with non-small cell lung cancer, Clin. Cancer Res. 19 (2013) 4273–4281, https://doi.org/10.1158/1078-0432.CCR-13-0318.

[8] A.T. Shaw, S.-H.I. Ou, Y.-J. Bang, D.R. Camidge, B.J. Solomon, R. Salgia, G.J. Riely, M. Varella-Garcia, G.I. Shapiro, D.B. Costa, R.C. Doebele, L.P. Le, Z. Zheng, W. Tan, P. Stephenson, S.M. Shreeve, L.M. Tye, J.G. Christensen, K.D. Wilner, J.W. Clark, A.J. Iafrate, Crizotinib in ROS1 -rearranged non–Small-cell lung cancer, N. Engl. J. Med. 371 (2014) 1963–1971, https://doi.org/10.1007/s00406-014-0563-z.

[9] K. Takeuchi, M. Soda, Y. Togashi, R. Suzuki, S. Sakata, S. Hatano, R. Asaka, W. Hamanaka, H. Ninomiya, H. Uehara, Y. Lim Choi, Y. Satoh, S. Okumura, K. Nakagawa, H. Mano, Y. Ishikawa, RET, ROS1 and ALK fusions in lung cancer, Nat. Med. 18 (2012) 378–381, https://doi.org/10.1038/nm.2658.

[10] L. Sholl, H. Sun, M. Butaney, ROS1 immunohistochemistry for detection of ROS1-rearranged lung adenocarcinomas, Am. J. 37 (2013) 1441–1449 http://europepmc.org/abstract/MED/23887156.

[11] A. Yoshida, T. Kohno, K. Tsuta, S. Wakai, Y. Arai, Y. Shimada, H. Asamura, K. Furuta, T. Shibata, H. Tsuda, ROS1-rearranged lung cancer, Am. J. Surg. Pathol. 37 (2013) 554–562, https://doi.org/10.1097/PAS.0b013e3182758fe6.

[12] S.E. Lee, B. Lee, M. Hong, J.Y. Song, K. Jung, M.E. Lira, M. Mao, J. Han, J. Kim, Y. La Choi, Comprehensive analysis of RET and ROS1 rearrangement in lung adenocarcinoma, Mod. Pathol. 28 (2015) 468–479, https://doi.org/10.1038/modpathol.2014.107.

[13] H. Go, D.W. Kim, D. Kim, B. Keam, T.M. Kim, S.H. Lee, D.S. Heo, Y.J. Bang, D.H. Chung, Clinicopathologic analysis of ros1-rearranged non-small-cell lung cancer and proposal of a diagnostic algorithm, J. Thorac. Oncol. 8 (2013) 1445–1450, https://doi.org/10.1097/JTO.0b013e3182a4dd6e.

[14] Y. Pan, Y.Y. Zhang, Y. Li, H. Hu, L. Wang, H. Li, R. Wang, T. Ye, X. Luo, Y.Y. Zhang, B. Li, D. Cai, L. Shen, Y. Sun, H. Chen, ALK, ROS1 and RET fusions in 1139 lung adenocarcinomas: a comprehensive study of common and fusion pattern-specific clinicopathologic, histologic and cytologic features, Lung Cancer. 84 (2014) 6–11, https://doi.org/10.1016/j.lungcan.2014.02.007.

[15] Y. Jin, P.-L. Sun, S.Y. Park, H. Kim, E. Park, G. Kim, S. Cho, K. Kim, C.-T. Lee, J.-H. Chung, Frequent aerogenous spread with decreased E-cadherin expression of ROS1- rearranged lung cancer predicts poor disease-free survival, Lung Cancer. 89 (2015) 343–349, https://doi.org/10.1016/j.lungcan.2015.06.012.

[16] J.J. Lin, A.T. Shaw, Recent advances in targeting ROS1 in lung cancer, J. Thorac. Oncol. 12 (2017) 1611–1625, https://doi.org/10.1016/j.jtho.2017.08.002.

[17] L. Mescam-Mancini, S. Lantuéjoul, D. Moro-Sibilot, I. Rouquette, P.J. Souquet, C. Audigier-Valette, J.C. Sabourin, C. Decroisette, L. Sakhri, E. Brambilla,

A. McLeer-Florin, On the relevance of a testing algorithm for the detection of ROS1-rearranged lung adenocarcinomas, Lung Cancer. 83 (2014) 168–173, https://doi.org/10.1016/j.lungcan.2013.11.019.
[18] J. Zhao, X. Chen, J. Zheng, M. Kong, B. Wang, W. Ding, A genomic and clinicopathological study of non-small-cell lung cancers with discordant ROS1 gene status by fluorescence in-situ hybridisation and immunohistochemical analysis, Histopathology. 73 (2018) 19–28, https://doi.org/10.1111/his.13492.
[19] J. Zhou, J. Zhao, J. Zheng, M. Kong, K. Sun, B. Wang, X. Chen, W. Ding, J. Zhou, A prediction model for ROS1-rearranged lung adenocarcinomas based on histologic features, PLoS One. 11 (2016) 1–12, https://doi.org/10.1371/journal.pone.0161861.
[20] A. Warth, T. Muley, C. Kossakowski, A. Stenzinger, P. Schirmacher, H. Dienemann, W. Weichert, Prognostic impact and clinicopathological correlations of the cribriform pattern in pulmonary adenocarcinoma, J. Thorac. Oncol. 10 (2015) 638–644, https://doi.org/10.1097/JTO.0000000000000490.
[21] K. Tsuta, G. Ishii, K. Yoh, J.I. Nitadori, T. Hasebe, Y. Nishiwaki, Y. Endoh, T. Kodama, K. Nagai, A. Ochiai, Primary lung carcinoma with signet-ring cell carcinoma components: clinicopathological analysis of 39 cases, Am. J. Surg. Pathol. 28 (2004) 868–874, https://doi.org/10.1097/00000478-200407000-00004.
[22] M.B. Amin, P. Tamboli, S.H. Merchant, N.G. Ordóñez, J. Ro, A.G. Ayala, J.Y. Ro, Micropapillary component in lung adenocarcinoma: a distinctive histologic feature with possible prognostic significance, Am. J. Surg. Pathol. 26 (2002) 358–364 (accessed December 4, 2018), http://www.ncbi.nlm.nih.gov/pubmed/11859208.
[23] W.D. Travis, E. Brambilla, A.G. Nicholson, Y. Yatabe, J.H.M. Austin, M.B. Beasley, L.R. Chirieac, S. Dacic, E. Duhig, D.B. Flieder, K. Geisinger, F.R. Hirsch, Y. Ishikawa, K.M. Kerr, M. Noguchi, G. Pelosi, C.A. Powell, M.S. Tsao, I. Wistuba, WHO panel, the 2015 world health organization classification of lung tumors, J. Thorac. Oncol. 10 (2015) 1243–1260, https://doi.org/10.1097/JTO.0000000000000630.
[24] Y. Nakazato, A.M. Maeshima, Y. Ishikawa, Y. Yatabe, J. Fukuoka, T. Yokose, Y. Tomita, Y. Minami, H. Asamura, K. Tachibana, T. Goya, M. Noguchi, Interobserver agreement in the nuclear grading of primary pulmonary adenocarcinoma, J. Thorac. Oncol. 8 (2013) 736–743, https://doi.org/10.1097/JTO.0b013e318288dbd8.
[25] I. Petersen, W.F.M.A. Kotb, K.-H. Friedrich, K. Schlüns, A. Böcking, M. Dietel, Core classification of lung cancer: correlating nuclear size and mitoses with ploidy and clinicopathological parameters, Lung Cancer. 65 (2009), https://doi.org/10.1016/j.lungcan.2008.12.013 312–8..
[26] Y. Nakazato, Y. Minami, H. Kobayashi, K. Satomi, Y. Anami, K. Tsuta, R. Tanaka, M. Okada, T. Goya, M. Noguchi, Nuclear grading of primary pulmonary adenocarcinomas, Cancer. 116 (2010) 2011–2019, https://doi.org/10.1002/cncr.24948.
[27] J.A. Barletta, B.Y. Yeap, L.R. Chirieac, Prognostic significance of grading in lung adenocarcinoma, Cancer. 116 (2010) 659–669, https://doi.org/10.1002/cncr.24831.
[28] H. Kim, S.J. Jang, D.H. Chung, S.B. Yoo, P. Sun, Y. Jin, K.H. Nam, J.H. Paik, J.H. Chung, A comprehensive comparative analysis of the histomorphological features of ALK-rearranged lung adenocarcinoma based on driver oncogene mutations: frequent expression of epithelial-mesenchymal transition markers than other genotype, PLoS One. 8 (2013), https://doi.org/10.1371/journal.pone.0076999.
[29] A. Yoshida, K. Tsuta, S. ichi Watanabe, I. Sekine, M. Fukayama, H. Tsuda, K. Furuta, T. Shibata, Frequent ALK rearrangement and TTF-1/p63 co-expression in lung adenocarcinoma with signet-ring cell component, Lung Cancer. 72 (2011) 309–315, https://doi.org/10.1016/j.lungcan.2010.09.013.
[30] A. Sonzogni, F. Bianchi, A. Fabbri, M. Cossa, G. Rossi, A. Cavazza, E. Tamborini, F. Perrone, A. Busico, I. Capone, B. Picciani, B. Valeri, U. Pastorino, G. Pelosi, Pulmonary adenocarcinoma with mucin production modulates phenotype according to common genetic traits: a reappraisal of mucinous adenocarcinoma and colloid adenocarcinoma, J. Pathol. Clin. Res. 3 (2017) 139–152, https://doi.org/10.1002/cjp2.67.
[31] H.S. Shim, Z. Mari-Kenudson, M. Zheng, Y.J. Liebers, Q.H. Cha, M. Ho, L.P. Onozato, R.S. Le, A. Heist, John Iafrate, Unique genetic and survival characteristics of invasive mucinous adenocarcinoma of the lung, J. Thorac. Oncol. 10 (2015) 1156–1162, https://doi.org/10.1097/JTO.0000000000000579.
[32] C.I. Selinger, B.T. Li, N. Pavlakis, M. Links, A.J. Gill, A. Lee, S. Clarke, T.N. Tran, T. Lum, P.Y. Yip, L. Horvath, B. Yu, M.R.J. Kohonen-Corish, S.A. O'Toole, W.A. Cooper, Screening for ROS1 gene rearrangements in non-small-cell lung cancers using immunohistochemistry with FISH confirmation is an effective method to identify this rare target, Histopathology. 70 (2017) 402–411, https://doi.org/10.1111/his.13076.
[33] A. Yoshida, K. Tsuta, S. Wakai, Y. Arai, H. Asamura, T. Shibata, K. Furuta, T. Kohno, R. Kushima, Immunohistochemical detection of ROS1 is useful for identifying ROS1 rearrangements in lung cancers, Mod. Pathol. 27 (2014) 711–720, https://doi.org/10.1038/modpathol.2013.192.